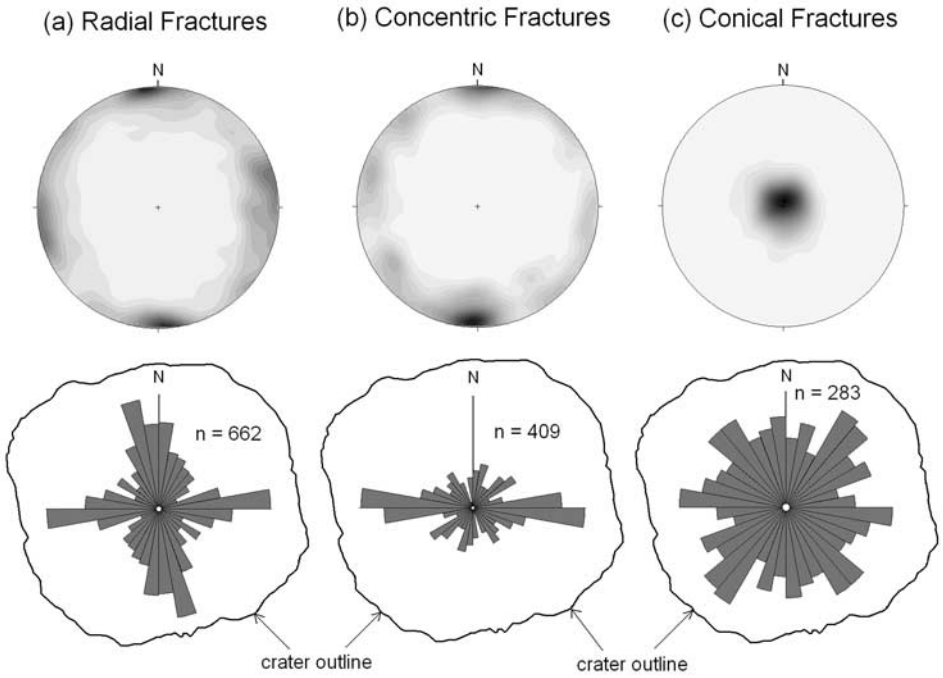

Figure 12. Equal-area plots of pole density contours and bidirectional rose diagrams displaying the geometry of impact fractures, when the bedding surfaces are restored to the horizontal surface, similar to the preimpact target conditions. (a) Note that the geometry of the radial fractures is more or less parallel to the straight walls of the crater, suggesting their production was affected by the same preimpact fracture system that is responsible for the near-squarish outline of the crater. (b) The concentric fractures have an approximately E-W preferred orientation, similar to one of the dominant orientations of the preimpact fractures. (c) The conical fractures show a radial pattern dissimilar to the preimpact fractures and, therefore, appear to be an independent impact-related product; the NW-SE and NE-SW conical fractures are subparallel to the major tear faults occurring in the crater diagonals.

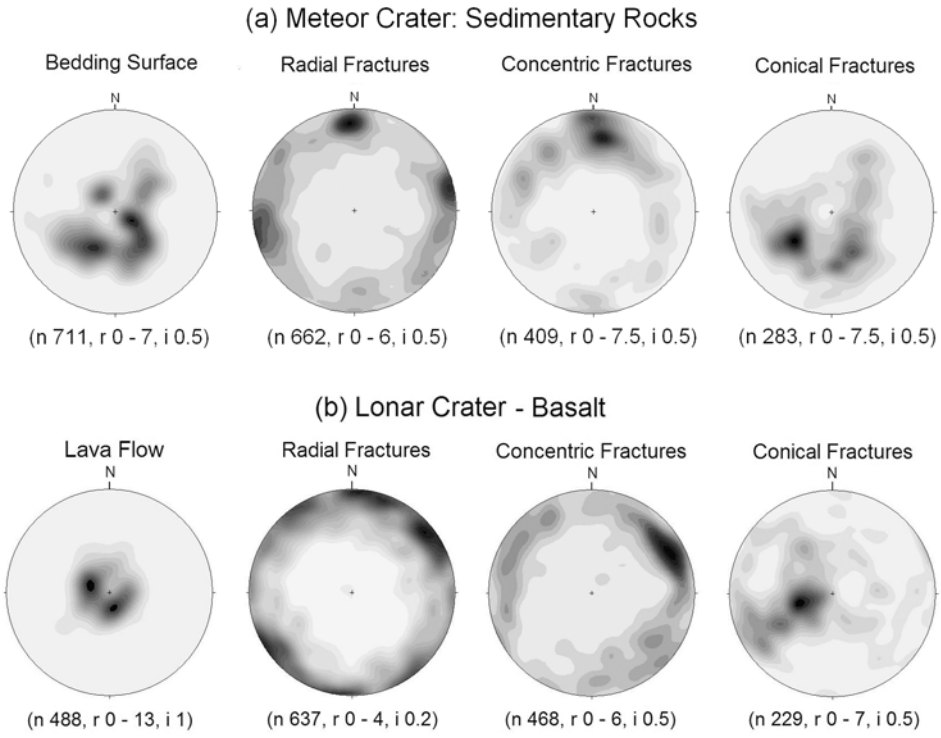

Figure 13. A comparison between the impact structures of (a) Meteor Crater and (b) Lonar Crater. Number of strike/dip measurements (n); pole density range in percent (r); and contour interval in percent (i).